

PIECEWISE LINEAR MODEL FOR REAL-TIME RATE CONTROL

Chi-Wah Wong*, Oscar C. Au, Raymond Chi-Wing Wong⁺, Hong-Kwai Lam

Hong Kong Univ. of Science and Technology, Hong Kong ⁺the Chinese University of Hong Kong, Hong Kong

Email: {dickywcw*, eeau, eekwai}@ust.hk

Email: {cwwong@cse.cuhk.edu.hk}

ABSTRACT

Most of existing rate control schemes in the literature evaluate quantization parameters of macro-blocks (MB) based on the models estimating well at low bit rates (e.g. quadratic model). These models are not flexible because this model does not estimate well for different situations with different rates. This work investigates the relationships of the rate and the distortion of a residue MB with two parameters -- MB quantization step size and standard deviation of MB prediction errors. Piecewise linear rate model and linear distortion model are proposed. Then we present the proposed rate control scheme based on these models. The experimental results suggest that our scheme achieves PSNR gain over TMN8 and Li's scheme.

1 Introduction

The rate control is used to prevent the buffer from over-flowing (resulting in frame skipping) or/and under-flowing (resulting in low channel utilization) in order to achieve good video quality. This can be done by minimizing the mean-square error (MSE) or maximum distortion subject to the rate constraint ([8], [9]). However, these approaches are generally not suitable for real-time encoding due to their high complexities. For real-time video communications such as video conferencing, it is more challenging as the rate control requires satisfying the low-delay constraint, especially in low bit rate channels. TMN8 rate control algorithm updates the model parameters in macro-block level [1]. TMN8 has better performance compared with some existing real-time rate control methods. However, TMN8 uses quadratic rate model estimating well at low bit rates. It is not suitable for TMN8 to work well at all bit rates. At high bit rates, the modeling may not be as good as that at low bit rates. Similar result occurs in [7] as this scheme also uses quadratic rate model alone. So, they cannot be scalable at all bit rates.

In this work, we present a simple, efficient model-based rate control scheme for encoders in real-time video communications. This work focuses on doing rate control for inter-coded frames (i.e. P-frame), which is used mostly in low-delay video communication. In this paper, the framework of our approach is shown as follows. Firstly, the piecewise linear rate model (by using 3 line segments for more accurate modeling) with the factor of the standard deviation of MB prediction errors is proposed based on our observation of entropy function. Secondly, another model - the distortion model - is also proposed based on our observation of MSE distortion function. This distortion model avoids updating its parameters in our scheme, making the complexity of our scheme lower. After obtaining rate and distortion models, we are going to minimize the objective function in the distortion model subject to the target bit constraint by using Lagrange optimization. Some formulas are then derived and are used to find the quantization parameters in order to encode frames with high quality.

This paper is organized as follows. We are going to describe the rate and distortion models in sections 2 and 3

respectively. In section 4, we obtain the optimal quantization step size that we minimize MSE distortion subject to the target bit constraint. In section 5, our rate control scheme is described. In section 6, the experiments are conducted to evaluate the performance. Finally, the conclusion is made.

2 Rate Model for the residue frame

We are going to describe the entropy per pixel in Sub-section 2.1 and propose our rate model per pixel in Sub-section 2.2.

2.1 Theoretical Expression for Entropy

In DCT-based motion compensated video encoders, the current video frame to be encoded is decomposed into 16x16 macroblocks (MB). Motion estimation and compensation are applied to give the residue MB, each of which is divided into sixteen 4x4 blocks and discrete cosine transform is applied to the 4x4 residue blocks in H.264 [4]. After that, the DCT coefficients within a block are quantized, zigzag scanned and encoded with variable length coding in general. The number of encoded bits and distortion of a given MB are observed to be dependent on the MB's quantization step size Q and the standard deviation σ of the residue MB.

By the motion prediction process, the pixel values of the residue MB tend to have Laplacian probability density function with standard deviation σ . The entropy H of the uniformly-quantized residue DCT coefficients is given by [6]:

$$H(\alpha) = -\left(1 - \exp\left(-\frac{\alpha}{2}\right)\right) \log_2\left(1 - \exp\left(-\frac{\alpha}{2}\right)\right) - 2 \sinh\left(\frac{\alpha}{2}\right) \left\{ \log_2\left(\sinh\left(\frac{\alpha}{2}\right)\right) \frac{1}{e^{\alpha} - 1} + \frac{\alpha}{\ln 2} \frac{-e^{\alpha}}{(e^{\alpha} - 1)^2} \right\} \quad (1)$$

where $\alpha = \sqrt{2}Q/\sigma$, Q is the quantization step size. The solid line in Figure 1 shows theoretical entropy. The solid-line curve is quadratic-like when σ/Q is small (e.g. 0 - 0.25). The curve is linear-like when σ/Q is larger (e.g. 0.25 - 1). The curve is log-like when σ/Q is much larger (e.g. > 1). As the actual rate is more or less related to the entropy function, the rate can be modeled from the entropy function [1].

It is noted that H is the function of α only. Due to the high complexity of Eq. (1), the actual expression is not used. Instead, an approximation is made to simplify the theoretical expression of Eq. (1). A simplified form $H(\sigma/Q)$ was presented in [1]. A simplified curve is quadratic for small σ/Q and log-like for large σ/Q . Figure 1 also shows the comparison of the theoretical entropy per pixel with the approximated curve when $QP = 35$. Some rate control schemes use the quadratic model ([1], [7]) while some rate control schemes use the log model. In the following, we will introduce a piecewise linear rate model instead. To our best knowledge, it is the first time to propose a linear rate control model in the area of rate control.

2.2 Rate Model

As discussed above, the analytical form of the entropy is the function of σ/Q only (i.e. α). The linear function of σ/Q can be used to approximate the actual form of entropy. It is easy to observe that there exist three regions (namely Region 1, Region 2 and Region 3 (counting from left to right)) with

large different slopes in Figure 1 (i.e. the case where σ/Q is small, the case where σ/Q is medium, and the case where σ/Q is large). Therefore, piecewise-linear functions can be a good approximation of $H(\sigma/Q)$. The piecewise approximation of the rate per pixel (called normalized rate) by using 3 straight line segments is shown as follows:

$$R' = \begin{cases} K_1 \frac{\sigma}{Q} & \text{when } 0 \leq \frac{\sigma}{Q} < \frac{L_2}{K_1 - K_2} \\ K_2 \frac{\sigma}{Q} + L_2 & \text{when } \frac{L_2}{K_1 - K_2} \leq \frac{\sigma}{Q} < \frac{L_3 - L_2}{K_2 - K_3} \\ K_3 \frac{\sigma}{Q} + L_3 & \text{otherwise} \end{cases} \quad (2)$$

where K_1, K_2, K_3, L_2, L_3 are model parameters for the rate model. It is noted that the greater the number of line segments we use, the higher the accuracy of the rate estimation. The range of each region depends on the intersection between two line segments for rate modeling. For instance, region 1 is in the range of σ/Q between 0 and $L_2/(K_1 - K_2)$. $L_2/(K_1 - K_2)$ is the intersection point between line segments in regions 1 and 2.

Figure 2 shows how these three line segments are intersected to form three regions. The left hand side of Figure 2 is a zoom-in view of the intersection of the first two line segments for small σ/Q whereas the right hand side of Figure 2 shows the intersection of the second and third line segments for large σ/Q .

3 Distortion Model for the residue frame

We are going to describe the MSE (Mean Square Error) distortion per pixel in Sub-section 3.1 and propose our distortion model in Sub-section 3.2.

3.1 Theoretical Expression for Distortion

The distortion is introduced by uniformly quantizing DCT coefficients with a quantizer. The MSE (Mean Square Error) distortion D after uniform quantization is given by [8]:

$$D = \sigma^2 - \exp\left(\frac{-\sqrt{2}Q}{2\sigma}\right) \left[\frac{Q^2}{4} + \frac{\sigma Q}{\sqrt{2}} + \sigma^2 \right] + \frac{2}{\exp\left(\frac{\sqrt{2}Q}{\sigma}\right) - 1} \left[\frac{Q^2}{4} \sinh\left(\frac{\sqrt{2}Q}{2\sigma}\right) - \frac{\sigma Q}{\sqrt{2}} \cosh\left(\frac{\sqrt{2}Q}{2\sigma}\right) + \sigma^2 \sinh\left(\frac{\sqrt{2}Q}{2\sigma}\right) \right] \quad (3)$$

It is noted that D is the function of σ and Q (not Q/σ or α) which is different from the entropy H . The distortion term increases with σ in general. In addition, the distortion increases with quantization step size Q .

3.2 Distortion Model

Similar to the theoretical expression of H , because the expression D has very high computational complexity, an approximation is made to simplify the actual expression. We propose the following function D' to approximate the D function by the following general model:

$$D' = a\sigma Q^c + b \quad (4)$$

where a, b , and c are real numbers ($a, c \geq 0$; b can be positive or negative). If $a=1/12$, $b=2$ and $c=0$, Eq. (4) becomes the distortion model of TMN8 [1] at low bit rates (i.e. bpp (bit per pixel) $= B/AN \rightarrow 0$).

Similar to the original function D , D' increases with σ and Q . It is known that the distortion is equal to $Q^2/12$ for uniform data distribution [1]. When the distribution is non-uniform (e.g. Laplacian), the distortion is not only dependent on Q , but also σ . [1] and [8] states that the distortion increases with σ . The rationale of our proposed distortion is based on our observation of the relationship between distortion and two terms σ and Q^c . The distortion increases with σ and Q^c . Although D' is not like the theoretical function D and D' is not derived from D mathematically (as in [3]), this simplified

expression provides other important properties for video encoders. As discussed later, the optimal quantization step size in our model is independent of the factors a, b and c . This means that a, b and c are not needed to be updated. So, we do not care about the values of a, b and c . Some previous works (e.g. [3]) propose the distortion model derived from D with some approximations, obtaining few advantages. Such model requires computation-demanding operations to update the model parameters due to the high complexity function of such kind of model.

4 Quantization Step Size Optimization

In this section, we derive formulas for the optimal quantization step size Q^* to minimize MSE distortion subject to the target bit constraint based on our models (i.e. Eq. (2) and Eq. (4)).

The quantization step sizes are chosen based on the optimization formula like [1]. The original problem is

$$Q_1^*, Q_2^*, \dots, Q_N^* = \arg \min_{Q_1, Q_2, \dots, Q_N} \frac{1}{N} \sum_{i=1}^N D_i \quad (5)$$

where Q_i^* is the optimal quantization step size of the i -th MB, B is the target number of bits for the frame, and N is the number of MB of the frame.

By using Lagrange techniques, the problem becomes

$$Q_1^*, Q_2^*, \dots, Q_N^*, \lambda = \arg \min_{Q_1, Q_2, \dots, Q_N, \lambda} \left\{ \frac{1}{N} \sum_{i=1}^N D_i + \lambda \left[\sum_{i=1}^N R_i - B \right] \right\} \quad (6)$$

By substituting D_i and R_i ,

$$Q_1^*, Q_2^*, \dots, Q_N^*, \lambda = \arg \min_{Q_1, Q_2, \dots, Q_N, \lambda} \left\{ \frac{1}{N} \sum_{i=1}^N (a\sigma_i Q_i^c + b) + \lambda \left[\sum_{i=1}^N A(K_j \frac{\sigma_i}{Q_i} + L_j + C) - B \right] \right\}$$

where A is the number of pixels in MB, C is the overhead rate.

By solving the above formula, the expression for the optimization quantization step size Q_i^* is

$$Q_i^* = \frac{AK_j^{1/(c+1)} \sum_{k=1}^N K_j^{c/(c+1)} \sigma_k}{B - ACN - A \sum_{k=1}^N L_j} \quad (7)$$

The new derived Eq. (7) contains parameter c . As we know, it is difficult for the user to adjust input parameters for good results. When this parameter c is needed to be inputted, other parameters a and b are also required and this will increase the encoder complexity. Besides, in Eq. (7), there is a computation of power operation inside the summation. It is quite resource-consuming in the encoder. From undesired properties of Eq. (7), we first assume that all MBs in a frame fall in a region. We will relax this assumption later. With this assumption, we obtain

$$Q_i^* = \frac{AK_j \sum_{k=1}^N \sigma_k}{B - AL_j N - ACN} \quad \text{in a given region} \quad (8)$$

It is observed that Q^* does not have the terms a, b and c . This implies that the terms a, b and c are not required to be updated in the distortion term D' . Only updating the model parameters (i.e. K_j and L_j) in the rate model is enough for the rate control. In other words, this equation has the low complexity (i.e. no need to update the model parameters in the distortion model) which is one of important factors in real-time rate control.

The assumption is quite reasonable when the majority of MBs in a frame fall in one region. The observation is described as follows. MBs usually falls in a group near to the origin of Figure 1. Different frames may vary the spread of

the MBs. So, MBs in a frame may fall in the region in three different possible cases.

- (1) All MBs fall in Region 1.
- (2) Some MBs fall in Region 1 and others fall in Region 2.
- (3) Each region contains some MBs in a frame.

We have two terms “classify” and “fall” to describe MBs. Each MB falls in Regions 1, 2 or 3. However, we classify each MB as four classes “Region 1”, “Region 2”, “Region 3” and “Zero Bit”. Table 1 shows the percentage of MBs classifying in classes Region 1, Region 2, Region 3 and “Zero Bit”. There is a column called “Zero Bit”, which corresponds to the percentage of MBs which is in the skip mode (i.e. the zero value of coded Block Pattern (CBP) indicates that no luminance and chrominance coefficients are required to be encoded [4]). If MBs are in the skip mode, they will be classified as “Zero Bit”, instead of the region they fall in. This is because MBs in the skip mode have the same distortion whatever the value of Q is. This means that this kind of MBs does not affect the method of choosing quantization step size. From Table 1, case 2 occurs frequently. The majority of frames in our tested video (e.g. slow-motion “Akiyo” and fast-motion “Stefan”) usually belong to the second case. MBs in Region 1 are usually in the skip mode because the encoder usually selects MBs with few number of encoded bits (usually in Region 1) as skip mode. As case 2 occurs frequently and MBs in Region 1 are usually in the skip mode, the majority of MBs except those in the skip mode in a frame is usually in Region 2. At higher bit rates, case 3 occurs. In this case, it is rare that MBs fall in Region 3 but most of MBs fall in Region 2. For example, in “Foreman” sequence with QP=5, MBs have 0%, 0.4%, 64.9% and 34.8% in “Zero Bit”, Region 1, Region 2 and Region 3 respectively. The majority of MBs in a frame is Region 2. At very low bit rates (e.g. QP=45), case 1 occurs more often and the majority of MBs in a frame is Region 1. This means that our assumption is valid in most of cases.

Besides, we have conducted experiments with the two following approaches:

- (1) All MBs in a frame use the same optimal Q expression (Eq. (8)), which belongs to the majority of MBs.
- (2) MBs use the optimal Q (Eq. (8)) in their corresponding region j. That is, MBs, corresponding different regions, uses different sets of optimal Q with K_j and L_j .

The results show that the second approach gives a better PSNR and the target bit rate can be achieved. These results may suggest that the minority of MBs should use the optimal Q expression (Eq.(8)) in their corresponding region to reach the rate-distortion optimal point. For the rest of the paper, we will use the second approach for our proposed rate control.

5. Tri-Linear Rate Control (TLRC)

In this section, we will introduce our proposed rate control algorithm. We assume that the first frame is intra-coded (I-frame) with a fixed quantization parameter and all subsequent frames are encoded as P-frames. This means that they are predicted from the corresponding previous decoded frames using motion compensation and the residue is obtained. First, we do the rate control in the frame layer, which is similar to TMN8. After that, we do the rate control in macro-block level.

I. Frame-Layer Rate Control

The encoder buffer size W is updated before the current frame is encoded with the following formula:

$$W = \max(W_{prev} + B' - R / F, 0) \quad (9)$$

where W_{prev} is the previous number of bits in the buffer, B' is the actual number of bits used for the encoded previous frame, R is the channel bit rate (bit per sec), and F is the frame rate (frame per sec).

After updating the buffer size, if W is larger than or equal to the predefined threshold M ($=R/F$), the encoder skips encoding the frames until W is smaller than M . This means that buffer overflow will not occur at the cost of frame skipping.

The target number of bits B for the current frame is estimated as:

$$B = (R/F) - \Delta \quad (10)$$

$$\text{where } \Delta = \begin{cases} W/F & W > 0.1M \\ W - 0.1M & \text{otherwise} \end{cases}$$

As the buffer size W keeps the low target buffer level (i.e. $0.1M$), which is very important in real-time rate control, the communication delay is very low.

II. Macro-block Layer Control

In H.264, quantization parameters are used in both rate control scheme and rate-distortion optimization (RDO), which results in the chicken and egg dilemma when rate control is used [7]. RDO gives residue information (e.g. MAD) from given QP whereas rate control gives desired QP from given residue information. In [7], this problem is solved by a prediction method based on residue information of the previous frame. The residue information of the current frame is predicted from that of the previous frame. In the following algorithm, we use average QP of the previous frame to predict residue information (i.e. σ_i) of the current frame, which is used in our rate control. In other words, the coding mode of each MB is determined based on the average QP of the previous frame. By doing this, σ_i of all MBs in the current frame can be obtained.

For each P-Frame

Compute all of σ_i

Compute $S_i = \sum_{n=1}^N \sigma_i$, $N_i=N$ and $B_i = B$

For each MB ($i = 1$ to N)

(1) Compute $Q_i = \frac{AK_i S_i}{B_i - AL_i N_i - ACN_i}$ based on Eq. (8)

(2) Use the corresponding QP to quantize and encode the i -th MB

(3) Compute $S_{i+1} = S_i - \sigma_i$, $N_{i+1}=N_i-1$ and $B_{i+1} = B_i - (\text{actual current bits})$

(4) Update the rate model parameters K_i and L_i based on Eq. (2)

(5) Update the overhead parameter C accordingly

The initialization is $K_1=0.32$, $K_2=1.4$, $L_2=-0.175$, $L_3=4$. Others (e.g. $L_1=0$ and $K_3=0.08$) are constant for simplicity in our rate control. All these values are found from Figure 2. The property of the second line is that the line should pass through $(\sigma_i/Q_i, R)=(0.125, 0)$ (See Figure 2) and then the relationship between L_2 and K_2 is $L_2 = -0.125K_2$. This means that K_1 , K_2 , L_2 , L_3 are needed to be updated (e.g. $K_1 = RQ_i/\sigma_i$, $K_2 = R/(\sigma_i/Q_i - 0.125)$, $L_2 = -0.125K_2$, $K_3 = (R - 4)Q_i/\sigma_i$). They will be updated further by averaging in a similar way in [1].

6. Experimental Results

We implemented the rate control scheme in a JVT JM 7.4 version. In the following experiments, we compare the proposed rate control algorithm with TMN8 [1] and a rate control [7], called Li, built in JM 7.4 which was released in Dec., 2003. Li rate control scheme is adopted in version JM 7.4 or higher. The first frame was intra-coded (I-frame) with $QP=31$, several frames were skipped after the first frame to decrease the number of bits in the buffer below $M=R/F$ and the remaining frames were all inter-coded (P frames). This means that the number of skipped frames is the same in

TMN8, Li and our proposed schemes (for fair comparison). Afterwards, they use their own schemes. The proposed algorithms, TMN8 and Li were simulated on some QCIF test sequences with a frame rate of 10fps and various target bit rates in a constant bit rate case. Here are the test conditions. The MV resolution is at 1/4 pel. Hadamard is “OFF”. RD optimization is “OFF”. Search range is “ ± 16 ”. Restrict search range is “0”. Reference frames is “1” and symbol mode is “UVLC”.

In our experiment, the actual encoded bit rates are achieved by TMN8, Li and the proposed rate control. They verify that these rate control methods can achieve a variety of target bit rates. The error between target bit rate and actual bit rate is below 0.2%. Table 3 shows the PSNR of the reconstructed pictures. A gain in PSNR by our proposed rate control over both TMN8 and Li is observed at all bit rates. This is because our piecewise linear rate model is more suitable than the alone quadratic rate model according to the empirical entropy of Q -quantized coefficient from Eq. (1). (TMN8 and Li uses quadratic rate model.) This can be verified from Table 2 as small model error (i.e. difference between the actual bits and predicted bits from the rate model of a MB) implies good modeling and better quality's results in general. In addition, as discussed before, the optimal quantization step size in our model is independent of the factors a , b and c . This means that a , b and c are not needed to be updated. So, we do not care about the values of a , b and c . Compared with Li, the complexity in our scheme is low. As discussed before, if $a=1/12$, $b=2$ and $c=0$, our distortion model becomes the distortion model of TMN8 at low bit rates. This fixed setting may not give a good distortion model in real encoders.

7. Conclusion

In this paper, linear rate model and linear distortion model with the factor of the standard deviation of residue MBs are established. Then we present the proposed rate control scheme based on these models. Our models are used by three line segments because the usage of segments can give a greater accuracy. The experimental results suggest that our scheme achieves PSNR gain over TMN8 and Li's scheme.

8. Acknowledgements

This work has been supported in part by the RGC grant HKUST6203/02E, and the ITF grant ITS/122/03 of the Hong Kong Special Administrative Region, China.

9. References

- [1] J. Ribas-Corbera and S. Lei, "Rate Control in DCT Video Coding for Low-Delay Communications", *IEEE Trans. Circuits Syst. Video Technol.*, vol. 9, pp.172-p.185, 1999
- [2] Z. He and S. K. Mitra, "A Linear Source Model and a Unified Rate Control Algorithm for DCT Video Coding", *IEEE Trans. Circuit Syst. Video Technol.*, vol. 12, pp. 970-982, 2002
- [3] Z. He and S. K. Mitra, "Zero-domain Bit Allocation and Rate Control for real time video coding", in *Proc. IEEE Int. Conf. Image Processing(ICIP)*, vol. 3, pp. 546-549, 2001
- [4] "H.264/MPEG-4 Part 10 Tutorials", <http://www.vcodels.fsnct.co.uk/h264.html>
- [5] H. J. Lee and T. H. Chiang and Y. Q. Zhang, "Scalable Rate Control for MPEG-4 Video", *IEEE Trans. Circuit Syst. Video Technol.*, vol. 10, pp. 878-894, 2000
- [6] F. Moscheni, F. Dufaux and H. Nicolas, "Entropy criterion for optimal bit allocation between motion and prediction error information", *Proc. SPIE Visual Commun. And Image Proc.*, pp. 235-242, Nov. 93
- [7] Z. G. Li, W. Gao, F. Pan, S. W. Ma, G. N. Feng, K. P. Lim, X. Lin, S. Rahardja, H. Lu and Yan Lu, "Adaptive Rate Control with HRD Consideration", ISO-IEC/JTC1/SC29/WG11/JVT-H014, Geneva, Switzerland, 20-26 May, 2003.
- [8] H.-M. Hang and J.-J. Chen, "Source Model for Transform Video Coder and Its Application – Part I: Fundamental Theory", *IEEE Trans.*

- Circuits Syst. Video Technol.*, vol. 7, pp. 287-298, 1997
- [9] J.-W. Lee, A. Vetro, Y. Wang and Y.-S. Ho, "Bit Allocation for MPEG-4 Video Coding With Spatio-Temporal Tradeoffs", *IEEE Trans. Circuits Syst. Video Technol.*, vol. 13, pp. 488-502, 2003

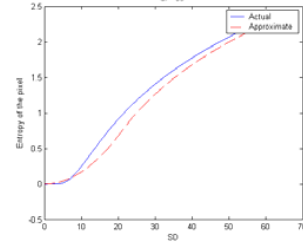


Figure 1: Comparison of the theoretical entropy per pixel (i.e. Eq. (1)) with the approximated curve when QP = 35

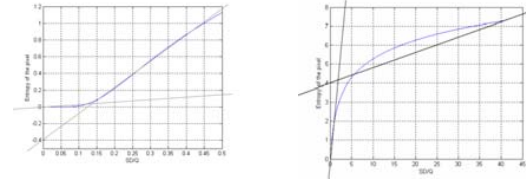


Figure 2: The magnified version of two approximation lines for small σ/Q and large σ/Q respectively

| Test Name | QP | Zero Bit (%) | Region 1 (%) | Region 2 (%) | Region 3 (%) |
|------------|----|--------------|--------------|--------------|--------------|
| Akiyo | 27 | 78.6 | 1.5 | 19.9 | 0.0 |
| Coastguard | 27 | 9.7 | 3.1 | 87.2 | 0.0 |
| Foreman | 27 | 23.8 | 2.3 | 73.9 | 0.0 |
| M & D | 27 | 61.8 | 37.8 | 0.4 | 0.0 |
| Stefan | 27 | 13.5 | 2.1 | 84.4 | 0.0 |
| Akiyo | 35 | 91.5 | 0.2 | 8.3 | 0.0 |
| Coastguard | 35 | 52.0 | 0.7 | 47.3 | 0.0 |
| Foreman | 35 | 53.7 | 0.5 | 45.8 | 0.0 |
| M & D | 35 | 84.1 | 15.8 | 0.1 | 0.0 |
| Stefan | 35 | 33.5 | 1.7 | 64.8 | 0.0 |

Table 1: Average percentage of MBs of a frame in corresponding regions for different QCIF sequences

| Test Name | Video Sequence | Tar.bit (kbps) | Rate Model Error per MB | | |
|-----------|----------------|----------------|-------------------------|-------|------|
| | | | TMN8 | Li | TLRC |
| Aki24 | Akiyo | 24 | 23.2 | 23.2 | 23.5 |
| Ctg256 | Coastguard | 256 | 135.8 | 102.8 | 54.4 |
| Fmn48 | Foreman | 48 | 24.2 | 23.6 | 23.5 |
| Fmn12 | Foreman | 128 | 69.8 | 62.6 | 44.4 |
| Mad24 | M & D | 24 | 17.9 | 17.2 | 17.2 |
| Stf256 | Stefan | 256 | 162.0 | 143.3 | 65.9 |
| Stf384 | Stefan | 384 | 338.3 | 289.2 | 89.6 |

Table 2: Comparison of the rate model error per MB achieved by TMN8, Li and TLRC

| Test Name | PSNR (dB) | | | PSNR gain over TMN8 | PSNR gain over Li |
|-----------|-----------|-------|-------|---------------------|-------------------|
| | TMN8 | Li | TLRC | | |
| Aki24 | 38.84 | 38.80 | 38.93 | +0.09 | +0.13 |
| Ctg256 | 37.17 | 37.31 | 37.51 | +0.34 | +0.2 |
| Fmn48 | 32.01 | 31.98 | 32.16 | +0.15 | +0.18 |
| Fmn12 | 36.63 | 36.90 | 37.41 | +0.78 | +0.51 |
| Mad24 | 35.85 | 35.80 | 35.93 | +0.08 | +0.13 |
| Stf256 | 33.52 | 33.45 | 34.08 | +0.56 | +0.63 |
| Stf384 | 36.47 | 36.38 | 36.91 | +0.44 | +0.53 |

Table 3: Comparison of PSNR achieved by TMN8, Li and TLRC